Synthesis, Crystal Structures, and Modifications of Novel Framework Gallium Diphosphonates

Howard G. Harvey,[†] Anne C. Herve,[‡] Helen C. Hailes,[‡] and Martin P. Attfield*[,§]

Davy-Faraday Research Laboratory, The Royal Institution of Great Britain, 21 Albemarle Street, London, W1S 4BS, U.K., Department of Chemistry, University College, University of London, 20 Gordon Street, London, WC1H 0AJ, U.K., and UMIST Centre for Microporous Materials, Department of Chemistry, UMIST, P.O. Box 88, Manchester, M60 1QD, U.K.

Received March 9, 2004. Revised Manuscript Received May 21, 2004

The framework gallium diphosphonates $Ga_2[O_3PC_2H_4PO_3](H_2O)_2F_2{\cdot}2H_2O$ (**1**) (triclinic, $P\bar{1}$, $a = 5.0432(2)$ Å, $b = 7.2468(3)$ Å, $c = 8.3499(4)$ Å, $\alpha = 107.489(2)°$, $\beta = 92.444(2)°$, $\gamma = 109.338(2)°$, $Z = 1$) and $Ga_2[O_3PCH_2(C_6H_4)CH_2PO_3](H_2O)_2F_2$ (**2**) (triclinic, $P\bar{1}$, $a = 4.9673(1)$ Å, $b = 7.0898(2)$ Å, $c = 10.1220(3)$ Å, $\alpha = 92.698(2)°$, $\beta = 93.153(2)°$, $\gamma = 109.122(2)°$, $Z = 1$) and the solid-solution series $Ga_2\{[O_3PCH_2(C_6H_4)CH_2PO_3]_{1-x}(HPO_3)_{2x}\}(H_2O)_2F_2$ ($0 \le x \le 0.146$) $x = 0.541$ (**3**) and $x = 0.144$ $Ga_2\{[O_3PCH_2(C_6H_4)CH_2PO_3]_{0.853(6)}(HPO_3)_{0.29(1)}\}(H_2O)_2F_2$ (**4**) (triclinic, $P\bar{1}$, $a = 4.959(2)$ Å, $b = 7.078(2)$ Å, $c = 10.024(3)$ Å, $\alpha = 92.404(5)°$, $\beta = 92.955(5)°$, $\gamma = 109.187(5)°$, $Z = 1$) have been synthesized by solvothermal methods and their structures determined using X-ray diffraction data. All the materials contain linear chains of corner-sharing GaO_4F_2 octahedra that are linked by the diphosphonate groups to form framework structures. The channels of **1** are found to contain two water molecules per unit cell while those in **2** are too narrow to contain extraframework species. The apertures created in the phosphite-substituted derivatives of **2** (**3** and **4**) are shown, by crystallographic methods, to be considerably larger than those in **2** and, by thermogravimetric methods, to create more open structures. The synthetic conditions or form of the diphosphonate group are found to play a defining role in the adoption of this particular configuration of the inorganic component in the reported compounds and provide an additional strategy for the rational design of framework hybrid organic−inorganic solids.

Introduction

The area of organic−inorganic hybrid materials is a rapidly expanding field of materials chemistry due to their novel properties and the potential for the rational design of their functionality and structure. One such group of hybrid materials that has received considerable interest is the metal phosphonate/diphosphonate family that has exhibited great possibilities for application in the areas of sorption,[1] ion exchange,[2,3] sensing,[4,5] charge storage,[6] and catalysis.[7,8]

The majority of work that has focused on the rational design of hybrid metal phosphonate materials has concentrated on controlling the form of the organic portion of the materials. This approach has included forming materials with progressively longer organic chains to increase the pore size of the resultant materials, for example, in the series of copper diphosphonates,[9−11] $Cu_2[(O_3P(CH_2)_2PO_3)(H_2O)_2]$, $Cu_2[(O_3P(CH_2)_3PO_3)(H_2O)_2]{\cdot}H_2O$, $Cu_2[(O_3P(CH_2)_4PO_3)(H_2O)_2]{\cdot}2H_2O$, $Cu_2[(O_3P(CH_2)_5PO_3)(H_2O)_2]{\cdot}2.8H_2O$, and $Cu_2[(O_3PCH_2(C_6H_4)CH_2PO_3)(H_2O)_2]$, titanium diphosphonates $Ti(O_3P(CH_2)_nPO_3)$ ($n = 2, 3$),[12] and rare-earth diphosphonates $LnH[O_3P(CH_2)_nPO_3]$ ($n = 1, 2, 3$),[13] or materials containing functionalizable groups, such as the zirconium 4,4′-biphenyl and 4,4′-terphenylbisphosphonates whose phenylene groups can be sulfonated to produce microporous materials containing strong Bronsted acid groups.[14]

Not only is it beneficial to control the size of pores through the length of the organic spacer but it is also desirable, particularly in framework pillared materials, to direct the interpillar spacing to produce materials with easy access to their internal volume. Thus, meth-

* To whom correspondence should be addressed. E-mail: m.attfield@umist.ac.uk. Tel: 00-44-161-200-4467. Fax: 00-44-161-200-4559.
[†] The Royal Institution of Great Britain.
[‡] University of London.
[§] UMIST.

(1) Maeda, K.; Kiyozumi, Y.; Mizukami, F. *J. Phys. Chem. B* **1997**, *101*, 4402.
(2) Yang, C. Y.; Clearfield, A. *React. Polym.* **1987**, *5*, 13.
(3) Kullberg, L. H.; Clearfield, A. *Solvent Extr. Ion. Exch.* **1989**, *7*, 527.
(4) Alberti, G.; Casciola, M.; Costantino, U.; Peraio, A.; Montoneri, E. *Solid State Ionics* **1992**, *50*, 315.
(5) Alberti, G.; Casciola, M. *Solid State Ionics* **1997**, *97*, 177.
(6) Vermeulen, L. A.; Thompson, M. E. *Nature* **1992**, *358*, 656.
(7) Deniaud, D.; Schollorn, B.; Mansuy, D.; Rouxel, J.; Battioni, P.; Bujoli, B. *Chem. Mater.* **1995**, *7*, 995.
(8) Maillet, C.; Janvier, P.; Pipelier, M.; Praveen, T.; Andres, Y.; Bujoli, B. *Chem. Mater.* **2001**, *13*, 2879.
(9) Poojary, D. M.; Zhang, B.; Clearfield, A. *J. Am. Chem. Soc.* **1997**, *119*, 12550.
(10) Arnold, D. I.; Ouyang, X.; Clearfield, A. *Chem. Mater.* **2002**, *14*, 2020.
(11) Riou, D.; Beler, F.; Serre, C.; Nogues, M.; Vichard, D.; Ferey, G. *Int. J. Inorg. Mater.* **2000**, *2*, 29.
(12) Serre, C.; Ferey, G. *Inorg. Chem.* **2001**, *40*, 5350.
(13) Serpaggi, F.; Ferey, G. *J. Mater. Chem.* **1998**, *8*, 2749.
(14) Wang, Z. K.; Heising, J. M.; Clearfield, A. *J. Am. Chem. Soc.* **2003**, *125*, 10375.

10.1021/cm049607v CCC: $27.50
Published on Web 08/25/2004

ods to increase, and control, the distance between the diphosphonate pillars and the porosity of the material have been pursued vigorously. Three methods to increase the interpillar separation have been reported. The first method involves pillaring the host material with a phosphate ester and a diphosphonic acid of similar dimensions and rendering the resultant material porous through hydrolysis of the phosphate ester to yield smaller P−OH groups.[15] The second method involves the controlled topotactic substitution of a fraction of the diphosphonate groups within a layered host, by smaller anions, for example, $H_2PO_4^-$ ions.[16] The final common method involves the formation of the porous material by coprecipitation of a metal species with the diphosphonic acid and a smaller spacer substituent $X-PO(OH)_2$, such as phosphorous acid (X = H). This methodology has been used to form several more open diphosphonate materials, including the solid solution aluminum phosphite/ethylenediphosphonate series, $Al_2[(O_3PC_2H_4PO_3)_{1-x}(HPO_3)_{2x}](H_2O)_2F_2{\cdot}H_2O$ ($0 \leq x \leq 0.32$)[17] and $Zr(HPO_3)_{1.2}(O_3PRPO_3)_{0.4}$ (R = 3,3′,5,5′-tetramethylbiphenyl).[18,19] The latter is a particularly noticeable example as the size of the base of the organic spacer directs the arrangement of the diphosphonate and phosphite groups.

All the aforementioned methods of increasing the pore size in these hybrid materials involve altering the form to the organic spacer or the density of organic pillars while keeping the inorganic component constant. However, controlling the structure of the inorganic portion of these hybrid materials is another route through which their pore architecture may be rationally designed. A simple way through which this type of control can be achieved is by preparing isostructural compounds with differently sized metal cations; for example, the pore size of the material, $M_2[O_3PC_2H_4PO_3](H_2O)_2F_2{\cdot}H_2O$, is increased by replacing the Al^{3+} cations for the larger Ga^{3+} cations and results in a noticeable effect on the reversible re-adsorption properties of the extraframework water in the system.[20,21] Another potential method to control the pore architecture in these materials is to alter the connectivity within the inorganic sections of the composite material to produce isomeric inorganic sections of different configuration but the same chemical formula.

In our continuing investigation of group 13 metal diphosphonate materials we have synthesized and structurally characterized the new materials $Ga_2[O_3PC_2H_4PO_3](H_2O)_2F_2{\cdot}2H_2O$ (**1**) and $Ga_2[O_3PCH_2(C_6H_4)CH_2PO_3](H_2O)_2F_2$ (**2**) that contain the same general framework structure $Ga_2[O_3PRPO_3](H_2O)_2F_2$. The framework of **1** is an isomeric form of the framework found in $Ga_2[O_3PC_2H_4PO_3](H_2O)_2F_2{\cdot}H_2O$,[20,21] but has a larger pore volume arising from the arrangement of the corner-sharing Ga-centered octahedra in the constituent inorganic chains in **1**. This connectivity of the Ga-centered octahedra is found to be controllable by modification of the synthetic conditions or the form of the diphosphonic acid molecules. By combining several of the techniques described above, we have synthesized directly and characterized the novel solid-solution series $Ga_2\{[O_3PCH_2(C_6H_4)CH_2PO_3]_{1-x}(HPO_3)_{2x}\}(H_2O)_2F_2$ ($0 \leq x \leq 0.146$) whose members contain potentially functionalizable groups and the largest aperture size within the family of group 13 metal diphosphonate materials. The structure of the $x = 0.147$ member (**4**) of this series, reported herein, represents the first structure determination using microcrystal X-ray crystallography of a member of a metal phosphite/diphosphonate solid-solution series.

Experimental Section

Materials and Methods. The reagents used to synthesize all the materials were $Ga_2(SO_4)_3{\cdot}18H_2O$ (Alfa Aesar), ethylenediphosphonic acid (Lancaster), phosphorous acid (Lancaster), HF/pyridine (70 wt %, Aldrich), pyridine (Aldrich) and 1,3-diaminopropane (Aldrich or BDH). [1,4-phenylenebis(methylene)]diphosphonic acid [$H_2O_3PCH_2(C_6H_4)CH_2PO_3H_2$] was prepared by formation of tetraethylene [1,4-phenylenebis(methylene)]diphosphonate [$(C_2H_5)_2O_3PCH_2(C_6H_4)CH_2PO_3(C_2H_5)_2$], using the method of Böhmer et al.,[22] and subsequent hydrolysis following the procedure of Ganguly et al.[23] All the reagents used to synthesize [1,4-phenylenebis(methylene)]diphosphonic acid were obtained from Aldrich and, like the aforementioned reagents, were used without further purification.

Microprobe, EDXA, measurements were used to determine the Ga:P ratio in compound **1**. Measurements were made in separate regions of the as-synthesized sample using an Oxford Instrument ISIS system (EDS) fitted with a JEOL 773 Superprobe operating with an accelerating voltage of 15 kV and a beam diameter of 2 μm, under a vacuum of 10^{-12} Torr.

The magic angle spinning solid-state nuclear magnetic resonance (MAS SSNMR) ^{31}P spectrum was recorded using a Bruker MSL 300 spectrometer for sample **2**. An 85% solution of H_3PO_4 was used as the reference with the spectrometer operating at a frequency of 121.50 MHz, a sample spinning speed of 20 kHz, and recycle delays of 30 s. The ^{19}F MAS NMR spectrum for **2** was recorded using a Bruker MSL 300 spectrometer operating at a frequency of 282.4 MHz and a sample spinning speed of 20 kHz, with recycle delays of 5 s and use of $CFCl_3$ as a reference. The ^{31}P MAS NMR spectra of the phosphite-substituted samples of **2** were collected using a Varian Unity Inova spectrometer operating at a frequency of 121.37 MHz and a sample spinning speed of 15 kHz, with recycle delays of 120 s and use of an 85% solution of H_3PO_4 as a reference.

Thermogravimetric analysis (TGA) data were collected using a Shimadzu TGA 50 thermogravimetric analyzer with the samples heated in open alumina crucibles under flowing nitrogen from 25 to 900 °C at a heating rate of 5 °C min^{-1}.

Room-temperature X-ray diffraction patterns were collected using a Siemens D500 diffractometer employing Ge-monochromated Cu $K\alpha_1$ radiation or a Phillips X'Pert diffractometer employing Cu $K\alpha_{1+2}$ radiation and a RTMS X'Celerator detector.

Sample Preparation. The sample of $Ga_2[O_3PC_2H_4PO_3](H_2O)_2F_2{\cdot}2H_2O$ (**1**) used for structure determination was synthesized by mixing together $Ga_2(SO_4)_3{\cdot}18H_2O$, ethylene-

(15) Dines, M. B.; Cooksey, R. E.; Griffith, P. C.; Lane, R. H. *Inorg. Chem.* **1983**, *22*, 1004.
(16) Alberti, G.; Marmottini, F.; Murciamascaros, S.; Vivani, R. *Angew. Chem., Int. Ed. Engl.* **1994**, *33*, 1594.
(17) Harvey, H. G.; Hu, J.; Attfield, M. P. *Chem. Mater.* **2003**, *15*, 179.
(18) Alberti, G.; Costantino, U.; Marmotti, F.; Vivani, R.; Zappelli, P. *Angew. Chem., Int. Ed. Engl.* **1993**, *32*, 1357.
(19) Alberti, G.; Costantino, U.; Marmottini, F.; Vivani, R.; Zapelli, P. *Microporous Mesoporous Mater.* **1998**, *21*, 297.
(20) Harvey, H. G.; Teat, S. J.; Attfield, M. P. *J. Mater. Chem.* **2000**, *10*, 2632.
(21) Attfield M. P.; Harvey, H. G. *Mater. Res. Soc. Symp. Proc.* **2000**, *658*, GG6.31.1.
(22) Bohmer, V.; Vogt, W.; Chafaa, S.; Meullemeestre, J.; Schwing, M. J.; Vierling, F. *Helv. Chim. Acta* **1993**, *76*, 139.
(23) Ganguly, S.; Mague, J. T.; Roundhill, D. M. *Inorg. Chem.* **1992**, *31*, 3500.

Table 1. Initial Synthesis Gel Compositions, Reaction Conditions, and Product Formulas of $Ga_2\{[O_3PCH_2(C_6H_4)CH_2PO_3]_{1-x}(HPO_3)_{2x}\}(H_2O)_2F_2$

H_3PO_3:$H_2O_3PCH_2(C_6H_4)CH_2PO_3H_2$:$Ga_2(SO_4)_3$·$18H_2O$:HF:pyridine[a]:$H_2O$: temperature (°C):time (d)	$Ga_2[(O_3PCH_2(C_6H_4)CH_2PO_3)_{1-x}(HPO_3)_{2x}](H_2O)_2F_2$[b]
0:2.25:1:17.3:109.4:288.6:150:4	$x = 0$ (**2**)
1.08:1.60:1:16.6:108.6:286:160:7	$x = 0.054(5)$ (**3**)
2.19:1.08:1:17.1:109.3:287:160:4	$x = 0.144(5)$ (**4**)

[a] Includes pyridine from HF/pyridine. [b] Formulas obtained from ^{31}P MAS SS NMR data.

diphosphonic acid, HF, pyridine, 1,3-diaminopropane, and deionized water to form a synthesis gel of molar ratio 1:2.44:9.8:61.6:15.1:162, which after stirring had an initial pH of 9.45. The reagent mixture was loaded in a 23 mL Teflon-lined steel autoclave and heated for 4 days at 200 °C. The crystalline product was washed and separated by suction filtration to reveal single crystals of several morphologies. EDXA analysis on the product showed that the different single-crystal morphologies had similar compositions, containing Ga:P in the ratio 1:1. The powder X-ray diffraction pattern of the bulk sample indicated that **1** was a minor phase formed in the presence of a, as yet unidentified, major phase. Repetition of the above synthesis for 11 d resulted in the formation of the unidentified phase. Repetition of the described synthesis in the absence of the 1,3-diaminopropane resulted in the formation of pure $Ga_2[O_3PC_2H_4PO_3](H_2O)_2F_2$·$H_2O$.[20,21]

A polycrystalline sample of $Ga_2[O_3PCH_2(C_6H_4)CH_2PO_3](H_2O)_2F_2$ (**2**) was prepared in a 23 mL Teflon-lined steel autoclave using the initial synthesis gel composition and reaction conditions outlined in Table 1. The [1,4-phenylenebis-(methylene)]diphosphonic acid was found to be only partially soluble in water; however, a clear gel was formed after the addition of pyridine and HF which, after stirring, had an initial pH of 6.65. The product was washed and separated by suction filtration to reveal a white powdered solid.

The solid-solution series of materials $Ga_2[(O_3PCH_2(C_6H_4)CH_2PO_3)_{1-x}(HPO_3)_{2x}](H_2O)_2F_2$ (**3**, **4**) was prepared in 23 mL Teflon-lined steel autoclaves using the initial synthesis gel compositions and reaction conditions outlined in Table 1. The ratio of phosphorous acid to diphosphonic acid in the synthesis gel was adjusted to 2:3 (**3**) and 2:1 (**4**) while keeping the total molar amount of phosphorus constant. The products were formed as a polycrystalline material (**3**) and as microcrystals (**4**) that were filtered and washed with distilled water and then acetone and dried at room temperature.

Single-Crystal Structure Determination of $Ga_2[O_3PC_2H_4PO_3](H_2O)_2F_2$·$2H_2O$ (1). A suitable crystal of compound **1** was mounted on a Nonius Kappa CCD diffractometer fitted with a Nonius FR591 rotating anode generator at the EPSRC National Crystallography Service, Southampton, U.K., and data were collected from it. The structure was solved by direct methods and refined by full-matrix least squares on F^2 using the SHELXS-97 and SHELXL-97 programs, respectively.[24,25] One of the electron density peaks within the framework structure, initially assigned as an oxygen atom, was reassigned as a fluorine atom to yield physically reasonable anisotropic atomic displacement parameters and to improve the final residual values. The occurrence of F atoms in the frameworks of these materials, and gallium fluorophosphates is common using this type of synthetic procedure.[17,20,21,26,27] The atomic displacement parameters of the non-hydrogen atoms were refined anisotropically. The hydrogen atoms of the ethyl groups and the bound water molecule were found from difference Fourier maps and were refined in riding mode. The hydrogen atoms of the extraframework water molecule were geometrically placed using the method of Nardelli and refined in riding mode.[28] The isotropic atomic displacement parameters of the hydrogen atoms were all restrained to have the same value during refinement. The crystallographic data and structure refinement parameters are summarized in the footnote,[29] atomic coordinates and equivalent isotropic and anisotropic atomic displacement factors are provided in the Supporting Information, and selected bond distances and angles are presented in Tables 3−5.

The void volume and solvent-accessible volume within **1** and $Ga_2[O_3PC_2H_4PO_3](H_2O)_2F_2$·$H_2O$[20,21] were calculated using the algorithm by Sluis and Spek[30] contained within the PLATON suite of programs[31] using the experimental structures from which the hydrogen atoms and extraframework water molecules were removed. This methodology has the effect of biasing the calculated void and solvent-accessible volumes toward higher values, but allows comparison of the values for the two different structures.

Ab Initio Powder X-ray Structure Determination of $Ga_2[O_3PCH_2(C_6H_4)CH_2PO_3](H_2O)_2F_2$ (2). The X-ray data used to determine the unit cell parameters of **2** were collected during a 12 h scan on a Siemens D500 X-ray diffractometer using Cu $K\alpha_1$ radiation ($\lambda = 1.54056$ Å). The first 20 low-angle Bragg reflections were used to determine the triclinic unit cell parameters using the auto-indexing programs KOHL[32] and LZON[33] contained within the CRYSFIRE suite of programs.[34] Synchrotron X-ray data were collected on a sample contained in a 0.5 mm diameter Lindemann glass capillary tube mounted on the high-resolution X-ray powder diffractometer at station 2.3, Daresbury, SRS, U.K. The incident X-ray wavelength was 1.25042 Å, selected using a Si(111) monochromator, and the capillary tube was spun during data collection to minimize preferred orientation and sampling effects. Data were collected with a step size of 0.01° 2θ for 3 s per step between 5 and 25° 2θ, 6 s per step between 25 and 50° 2θ, and 10 s per step between 50 and 90° 2θ. Corrections were made for synchrotron beam intensity decay through comparison with a beam flux monitor.

Structure factors were extracted from this diffraction data by the Le Bail method[35] as implemented in the GSAS suite of programs.[36] The background of the diffraction profile was fitted by a linear interpolation function fitted with 36 terms. The peak profiles were described by a pseudo-Voigt function with additional terms used to account for peak broadening effects.

(24) Sheldrick, G. M. *SHELXS-97, A Program for Crystal Structure Determination*; University of Göttingen: Göttingen, Germany, 1997.
(25) Sheldrick, G. M. *SHELXL-97, A Program for Crystal Structure Determination*; University of Göttingen: Göttingen, Germany, 1997.
(26) Harvey, H. G.; Slater, B.; Attfield, M. P. *Chem. Eur. J.* **2004**, accepted.
(27) Ferey, G. *J. Fluorine Chem.* **1995**, *72*, 187.
(28) Nardelli, M. *J. Appl. Crystallogr.* **1999**, *32*, 563.
(29) $GaPO_5CH_6$ (**1**), $M_W = 217.75$, crystal dimensions 0.06 × 0.03 × 0.02 mm, triclinic, space group $P\bar{1}$, $a = 5.0432(2)$ Å, $b = 7.2468(3)$ Å, $c = 8.3499(4)$ Å, $\alpha = 107.489(2)°$, $\beta = 92.444(2)°$, $\gamma = 109.338(2)°$, $V = 271.19(2)$ Å^3, $Z = 2$, $\rho_{calc} = 2.642$ g cm^{-3}, $\mu = 5.338$ mm^{-1}, $2\theta_{max} = 55.14°$, Mo Kα radiation $\lambda = 0.71073$ Å, ϕ and ω scans, $T = 120$ K, measured reflections 3439, independent reflections 1240, reflections included in refinement 1240, SORTAV absorption correction $T_{max} = 0.90$, $T_{min} = 0.74$, parameters refined = 87, R1 [$I > 4\sigma(I)$] = 0.044, R1 (all data) = 0.046, wR2 [$I > 4\sigma(I)$] = 0.1186, wR2 (all data) = 0.1201, $\Delta\rho_{max/min}$ 1.249 and −1.423 e Å^{-3}.
(30) Sluis, P. V. D.; Spek, A. L. *Acta Crystallogr. A* **1990**, *46*, 194.
(31) Spek, A. L. *PLATON−A Multipurpose Crystallographic Tool*; Utrecht University: Utrecht, The Netherlands, 2001.
(32) Louer, D. *Acta Crystallogr. A.* **1998**, *54*, 922.
(33) Shirley, R.; Louër, D. *Acta Crystallogr.* **1978**, *A34*, S382.
(34) Shirley, R. *The CRYSFIRE System for Automatic Powder Indexing: User's Manual*; The Lattice Press: 41 Guildford Park Avenue, Guildford, Surrey GU2 5NL, England, 1999.
(35) Le Bail, A.; Duroy, H.; Fourquet, J. *Mater. Res. Bull.* **1988**, *23*, 447.
(36) Von Dreele, R. B.; Larson, A. C. *GSAS, General Structure Analysis System*; Regents of the University of California: LANSCE, Los Alamos National Laboratory, 1995.

Table 2. Crystal Data and Structure Refinement Parameters for 2

formula	$GaPO_4FC_4H_6$
formula weight	237.73
temperature (K)	298
wavelength (Å)	1.25042
crystal system	triclinic
space group	$P\bar{1}$
a (Å)	4.9673(1)
b (Å)	7.0898(2)
c (Å)	10.1220(3)
α (deg)	92.698(2)
β (deg)	93.153(2)
γ (deg)	109.122(2)
V (Å^3)	335.5(1)
Z	2
ρ_{calc} (g cm^{-3})	2.264
no. of reflections	1019
no. of fitted parameters	81
R_p	0.0784
R_{wp}	0.1066
R_F	0.0320
χ^2	11.28

The extracted structure factors were used in the direct methods program SIRPOW97,[37] via the EXPO interface,[38] to provide the Ga, P, and some of the O atoms of the structure. Although the E-statistics given from the EXPO package suggested that the material possessed a center of symmetry, the space group $P1$ was used to generate the starting model. This model was used for the Rietveld refinement, again using the GSAS suite of programs.[36] The remaining atoms were located from difference Fourier maps with the aid of a series of heavily weighted soft constraints for the C−C bond distances of the phenyl ring. Inspection of the structure using the ADDSYM program, within the PLATON suite of programs,[31] revealed that the structure had the higher symmetry of $P\bar{1}$ and this symmetry was used to allow a final structure refinement with fewer refineable parameters.

During the initial cycles of Rietveld refinement soft constraints were applied to all the Ga−O, P−O/C, and C−C distances within the structure with the soft constraint weighting factor fixed at a high value. As the refinement proceeded, the soft constraint weighting factor was reduced to a final value of 5 for the latter cycles of the refinement. The final cycle of least-squares refinement included the histogram scale factor, zero point error, lattice parameters, background coefficients, peak profile parameters, and positional and isotropic atomic displacement parameters for all atoms in the structure. The isotropic atomic displacement parameters of all the atoms were restrained to have the same value during refinement. The final residuals and crystallographic data are given in Table 2, atomic coordinates and isotropic atomic displacement parameters are provided in the Supporting Information, and selected bond distances and angles are presented in Tables 3 and 4, respectively. The final observed, calculated, and difference profiles are shown in Figure 1.

Single-Crystal Structure Determination of $Ga_2\{[O_3PCH_2(C_6H_4)CH_2PO_3]_{0.853(6)}(HPO_3)_{0.29(1)}\}(H_2O)_2F_2$ (4). Single-crystal X-ray data were collected from a colorless, platelike single microcrystal of compound **4** mounted on a Bruker AXS SMART CCD diffractometer at the high-flux single-crystal diffraction station 9.8 at CCLRC, Daresbury Laboratory Synchrotron Radiation Source, U.K. The structure was solved in space group $P\bar{1}$ (in agreement with compound **2**) by direct methods and refined by full-matrix least squares using the SHELX programs.[24,25] All the hydrogen atoms of the water molecules and diphosphonate group were found from difference Fourier maps and refined in riding mode with all their atomic displacement parameters refined isotropically and restrained to have the same value during refinement. The atomic displacement parameters of all of the non-hydrogen atoms were refined anisotropically.

The incorporated phosphite groups possess the same geometry as the PO_3 groups of the diphosphonate linkages, making the presence of additional atomic sites due to the phosphite PO_3 species unlikely. This was found to be the case as no indication of split atomic sites or excessive residual electron density was found in the difference Fourier maps at the conclusion of the refinement. The incorporation of the phosphite group into the material may manifest itself in the structure refinement through both the location of the partially occupied site for the hydrogen atom of the phosphite moiety and a decrease in occupancy of the C atoms of the diphosphonate pillar. As previously stated, no residual electron density assignable to the hydrogen atom of the phosphite group was found in the difference Fourier maps at the conclusion of the refinement and so refinement of the occupancies of the C atoms of the diphosphonate group provide the correct final crystal structure and a method to determine the degree of phosphite substitution in the material. Initial free refinement of the occupancies of the C atoms together with their anisotropic atomic displacement parameters yielded values for the occupancies of the four crystallographically independent C atoms in the diphosphonate group of 0.78(2), 0.84(1), 0.86(1), and 0.87(1) and reasonable values for their anisotropic atomic displacement parameters. The C atom occupancies are of similar value, but must be equal in the real material, so in the final cycles of refinement the fractional occupancies of the C atoms, and the H atoms they are directly bound to, were restrained to have the same value during refinement. The crystallographic data and structure refinement parameters for compound **4** are given the footnote 39, atomic coordinates, equivalent isotropic, and anisotropic atomic displacement parameters are given in the Supporting Information, and selected bond distances and angles are presented in Tables 3−5.

Results and Discussion

Synthesis, Structure, and Pore Architecture of $Ga_2[O_3PC_2H_4PO_3](H_2O)_2F_2\cdot 2H_2O$ (1). Currently, compound **1** has only been synthesized, in the presence of 1,3-diaminopropane over a relatively short reaction period of 4 d, as the minor phase in the presence of a, as yet unidentified, major phase. Repetition of the above synthesis for a longer reaction time (11 d) resulted in the formation of the unidentified phase or, in the absence of 1,3-diaminopropane, resulted in the formation of pure $Ga_2[O_3PC_2H_4PO_3](H_2O)_2F_2\cdot H_2O$.[20,21] This indicates that the formation of compound **1** is favored in conditions of high pH (∼9.45) that result from the addition of 1,3-diaminopropane. The organic amine is not found within the final structure of **1** so presumably does not have a direct structure-directing effect in the formation of **1**. The fact that compound **1** is only present after relatively short reaction periods indicates that it is a kinetic product and that the unidentified phase, which results after a longer reaction period, is the thermodynamically favored product.

(37) Altomare, A.; Burla, M. C.; Camalli, M.; Cascarano, G.; Giacovazzo, C.; Guagliardi, A.; Moliterni, A. G. G.; Polidori, G.; Spagna, R. *SIRPOW97*; Istituto di Ricerca per lo Sviluppo di Metodologie Cristallografiche (IRMEC): Bari, Italy, 1997.

(38) Altomare, A.; Burla, M. C.; Camalli, M.; Carrozzini, B.; Cascarano, G.; Giacovazzo, C.; Guagliardi, A.; Moliterni, A. G. G.; Polidori, G.; Rizzi, R. *J. Appl. Crystallogr.* **1999**, *32*, 339.

(39) $Ga_2P_2F_2O_8C_{6.8}H_{10.8}$ (**4**), M_W = 460.25, crystal dimensions 0.06 × 0.05 × 0.04 mm, triclinic, space group $P1$, a = 4.959(2) Å, b = 7.078(2) Å, c = 10.024(3) Å, α = 92.404(5)°, β = 92.955(5)°, γ = 109.187(5)°, V = 331.2(2) Å^3, Z = 1, ρ_{calc} = 2.308 g cm^{-3}, μ = 4.373 mm^{-1}, $2\theta_{max}$ = 59.06°, synchrotron radiation λ = 0.6889 Å, ω scans, T = 150 K, measured reflections 3478, independent reflections 1782, reflections included in refinement 1782, SORTAV absorption correction T_{max} = 1.00, T_{min} = 0.89, parameters refined = 105, R1 [$I > 4\sigma(I)$] = 0.0281, R1 (all data) = 0.0324, wR2 [$I > 4\sigma(I)$] = 0.0736, wR2 (all data) = 0.0758, $\Delta\rho_{max/min}$ 0.721 and −1.117 e Å^{-3}.

Table 3. Selected Bond Distances (Å) for Compounds 1, 2, and 4

1[a]		**2**[b]		**4**[c]	
2 × Ga1−O3$^{\#4,\#5}$	1.936(3)	2 × Ga1−O1$^{\#1,\#2}$	1.969(7)	2 × Ga1−O1$^{\#2,\#3}$	1.945(2)
2 × Ga1−F1$^{\#6}$	1.941(2)	2 × Ga1−F1$^{\#1,\#2}$	1.891(5)	2 × Ga1−F1$^{\#1}$	1.931(2)
2 × Ga1−O2$^{\#6}$	1.953(3)	2 × Ga1−O4$^{\#3}$	1.954(6)	2 × Ga1−O4$^{\#1}$	1.930(2)
2 × Ga2−F1$^{\#7}$	1.942(2)	2 × Ga2−F1$^{\#4}$	1.916(6)	2 × Ga2−F1$^{\#4}$	1.880(1)
2 × Ga2−O1$^{\#7}$	1.958(3)	2 × Ga2−O2$^{\#4}$	2.041(7)	2 × Ga2−O2$^{\#4}$	2.031(2)
2 × Ga2−O4$^{\#7}$	2.022(4)	2 × Ga2−O3$^{\#4}$	1.906(7)	2 × Ga2−O3$^{\#2,\#5}$	1.894(2)
P1−O2$^{\#1}$	1.526(3)	P1−O1	1.536(7)	P1−O1	1.533(2)
P1−O1$^{\#2}$	1.526(3)	P1−O3	1.524(7)	P1−O3	1.531(2)
P1−O3	1.534(3)	P1−O4	1.596(7)	P1−O4	1.521(2)
P1−C1$^{\#3}$	1.801(4)	P1−C1	1.80(1)	P1−C1	1.784(3)
C1−C1$^{\#8}$	1.522(8)	C1−C2	1.52(1)	C1−C2	1.510(4)
		C2−C3	1.35(1)	C2−C3	1.400(4)
		C2−C4	1.39(1)	C2−C4	1.385(4)
		C3−C4$^{\#5}$	1.39(1)	C3−C4$^{\#6}$	1.386(4)

[a] For **1**: $^{\#1}x-1, y-1, z$. $^{\#2}-x-1, -y+1, -z$. $^{\#3}x, y-1, z$. $^{\#4}-x, -y+2, -z$, $^{\#5}x, y+1, z$. $^{\#6}-x, -y+3, -z$. $^{\#7}-x-1, -y+2, -z$. $^{\#8}-x-1, -y+3, -z+1$. [b] For **2**: $^{\#1}x-1, y, z$. $^{\#2}-x-1, -y-1, -z-1$. $^{\#3}-x, -y+1, -z+1$. $^{\#4}-x+1, -y, -z+1$. $^{\#5}-x, -y, -z$. [c] For **4**: $^{\#1}-x, -y+2, -z+2$. $^{\#2}-x+1, -y+2, -z+2$. $^{\#3}x-1, y, z$. $^{\#4}-x+1, -y+3, -z+2$. $^{\#5}x, y+1, z$. $^{\#6}-x, -y+1, -z+1$.

Table 4. Selected Bond Angles (deg) for Compounds 1, 2, and 4

1[a]		**2**[b]		**4**[c]	
O3$^{\#4}$−Ga1−O3$^{\#5}$	180.0	O1$^{\#1}$−Ga1−O1$^{\#2}$	180.0	O1$^{\#3}$−Ga1−O1$^{\#2}$	180.0
O3$^{\#4}$−Ga1−F1$^{\#6}$	93.6(1)	O1$^{\#1}$−Ga1−F1$^{\#1}$	94.0(3)	O1$^{\#3}$−Ga1−F1$^{\#1}$	94.86(7)
O3$^{\#5}$−Ga1−F1$^{\#6}$	86.4(1)	O1$^{\#1}$−Ga1−F1$^{\#2}$	86.0(3)	O1$^{\#3}$−Ga1−F1	85.14(7)
O3$^{\#4}$−Ga1−F1	86.4(1)	O1$^{\#1}$−Ga1−O4	85.9(3)	O1$^{\#3}$−Ga1−O4	87.36(7)
O3$^{\#5}$−Ga1−F1	93.6(1)	O1$^{\#1}$−Ga1−O4$^{\#3}$	94.1(3)	O1$^{\#3}$−Ga1−O4$^{\#1}$	92.64(7)
F1$^{\#6}$−Ga1−O1	180.0	O1$^{\#2}$−Ga1−F1$^{\#1}$	86.0(3)	O1$^{\#2}$−Ga1−F1$^{\#1}$	85.14(7)
O3$^{\#4}$−Ga1−O2$^{\#6}$	88.1(1)	O1$^{\#2}$−Ga1−F1$^{\#2}$	94.0(3)	O1$^{\#2}$−Ga1−F1	94.86(7)
O3$^{\#5}$−Ga1−O2$^{\#6}$	92.0(1)	O1$^{\#2}$−Ga1−O4	94.1(3)	O1$^{\#2}$−Ga1−O4	92.64(7)
F1$^{\#6}$−Ga1−O2$^{\#6}$	92.0(1)	O1$^{\#2}$−Ga1−O4$^{\#3}$	85.9(3)	O1$^{\#2}$−Ga1−O4$^{\#1}$	87.36(7)
F1−Ga1−O2$^{\#6}$	89.0(1)	F1$^{\#1}$−Ga1−F1$^{\#2}$	180.0	F1$^{\#1}$−Ga1−F1	180.0
O3$^{\#4}$−Ga1−O2	92.0(1)	F1$^{\#1}$−Ga1−O4	94.1(3)	F1$^{\#1}$−Ga1−O4	91.33(7)
O3$^{\#5}$−Ga1−O2	88.1(1)	F1$^{\#1}$−Ga1−O4$^{\#3}$	85.9(3)	F1$^{\#1}$−Ga1−O4$^{\#1}$	88.67(7)
F1$^{\#6}$−Ga1−O2	89.0(1)	F1$^{\#2}$−Ga1−O4	85.9(3)	F1−Ga1−O4	88.67(7)
F1−Ga1−O2	91.1(1)	F1$^{\#2}$−Ga1−O4$^{\#3}$	94.1(3)	F1−Ga1−O4$^{\#1}$	91.33(7)
O2$^{\#6}$−Ga1−O2	180.0	O4−Ga1−O4$^{\#3}$	180.0	O4−Ga1−O4$^{\#1}$	180.0
F1−Ga2−F1$^{\#7}$	180.0	F1−Ga2−F1$^{\#4}$	180.0	F1−Ga2−F1$^{\#4}$	180.0
F1−Ga2−O1	88.3(1)	F1−Ga2−O2	87.7(3)	F1$^{\#4}$−Ga2−O2$^{\#4}$	90.08(7)
F1$^{\#7}$−Ga2−O1	91.7(1)	F1−Ga2−O2$^{\#4}$	92.3(3)	F1−Ga2−O2$^{\#4}$	89.92(7)
F1−Ga2−O1$^{\#7}$	91.7(1)	F1−Ga2−O3	91.1(3)	F1$^{\#4}$−Ga2−O3$^{\#2}$	87.77(7)
F1$^{\#7}$−Ga2−O1$^{\#7}$	88.3(1)	F1−Ga2−O3$^{\#4}$	89.0(3)	F1−Ga2−O3$^{\#2}$	92.23(7)
O1−Ga2−O1$^{\#7}$	180.0	F1$^{\#4}$−Ga2−O2	92.3(3)	F1−Ga2−O2	90.08(7)
F1−Ga2−O4$^{\#7}$	89.9(1)	F1$^{\#4}$−Ga2−O2$^{\#4}$	87.7(3)	F1$^{\#4}$−Ga2−O2	89.92(7)
F1$^{\#}$7-Ga2−O4$^{\#7}$	90.1(1)	F1$^{\#4}$−Ga2−O3	89.0(3)	F1−Ga2−O3$^{\#5}$	87.77(7)
O1−Ga2−O4$^{\#7}$	90.2(1)	F1$^{\#4}$−Ga2−O3$^{\#4}$	91.1(3)	F1$^{\#4}$−Ga2−O3$^{\#5}$	92.23(7)
O1$^{\#7}$−Ga2−O4$^{\#7}$	89.8(1)	O2−Ga2−O2$^{\#4}$	180.0	O2−Ga2−O2$^{\#4}$	180.0
F1−Ga2−O4	90.1(1)	O2−Ga2−O3	90.0(4)	O2−Ga2−O3$^{\#2}$	91.14(8)
F1$^{\#7}$−Ga2−O4	89.9(1)	O2−Ga2−O3$^{\#4}$	90.0(4)	O2−Ga2−O3$^{\#5}$	88.86(8)
O1−Ga2−O4	89.8(1)	O2$^{\#4}$−Ga2−O3	90.0(4)	O2$^{\#4}$−Ga2−O3$^{\#2}$	88.86(8)
O1$^{\#7}$−Ga2−O4	90.2(1)	O2$^{\#4}$−Ga2−O3$^{\#4}$	90.0(4)	O2$^{\#4}$−Ga2−O3$^{\#5}$	91.14(8)
O4$^{\#7}$−Ga2−O4	180.0	O3−Ga2−O3$^{\#4}$	180.0	O3$^{\#2}$−Ga2−O3$^{\#5}$	180.0
O2$^{\#1}$−P1−O1$^{\#2}$	110.6(2)	O1−P1−O3	113.6(6)	O1−P1−O3	113.7(1)
O2$^{\#1}$−P1−O3	111.7(2)	O1−P1−O4	108.5(5)	O1−P1−O4	111.6(1)
O1$^{\#2}$−P1−O3	114.0(2)	O1−P1−C1	109.2(5)	O1−P1−C1	106.9(1)
O2$^{\#1}$−P1−C1$^{\#3}$	106.0(2)	O3−P1−O4	109.8(6)	O3−P1−O4	109.7(1)
O1$^{\#2}$−P1−C1$^{\#3}$	107.4(2)	O3−P1−C1	106.3(6)	O3−P1−C1	106.1(1)
O3−P1−C1$^{\#3}$	106.7(2)	O4−P1−C1	109.3(6)	O4−P1−C1	108.5(1)
C1$^{\#8}$−C1−P1$^{\#5}$	114.0(4)	P1−C1−C2	115(1)	P1−C1−C2	114.9(2)
		C1−C2−C3	120(2)	C1−C2−C3	120.7(3)
		C1−C2−C4	118(1)	C1−C2−C4	121.1(3)
		C3−C2−C4	122(1)	C3−C2−C4	118.2(3)
		C2−C3−C4$^{\#5}$	119(1)	C2−C3−C4$^{\#6}$	120.2(3)
		C2−C4−C3$^{\#5}$	119(1)	C2−C4−C3$^{\#6}$	121.6(3)

[a] For **1**: $^{\#1}x-1, y-1, z$. $^{\#2}-x-1, -y+1, -z$. $^{\#3}x, y-1, z$. $^{\#4}-x, -y+2, -z$. $^{\#5}x, y+1, z$. $^{\#6}-x, -y+3, -z$. $^{\#7}-x-1, -y+2, -z$. $^{\#8}-x-1, -y+3, -z+1$. [b] For **2**: $^{\#1}x+1, y, z$. $^{\#2}-x-1, -y-1, -z-1$. $^{\#3}-x, -y-1, -z-1$. $^{\#4}-x-1, -y, -z-1$. $^{\#5}-x, -y, -z$. [c] For **4**: $^{\#1}-x, -y+2, -z+2$. $^{\#2}-x+1, -y+2, -z+2$. $^{\#3}x-1, y, z$. $^{\#4}-x+1, -y+3, -z+2$. $^{\#5}x, y+1, z$. $^{\#6}-x, -y+1, -z+1$.

The structure of $Ga_2[O_3PC_2H_4PO_3](H_2O)_2F_2{\cdot}2H_2O$ (**1**) is shown in Figure 2a and b. The structure consists of chains of corner-sharing GaO_4F_2 octahedra with bridging fluorine atoms (F1) linking the octahedra as shown in Figures 2a and 3. These chains consist of two types of GaO_4F_2 octahedra that both contain gallium atoms coordinated to two fluorine atoms in a trans configuration. The remaining corners of one of the gallium-centered octahedra (Ga1) are occupied by four oxygen atoms (O2 and O3) from four different diphosphonate groups, while the remaining apexes of the other gallium-centered octahedra (Ga2) are occupied by two oxygen

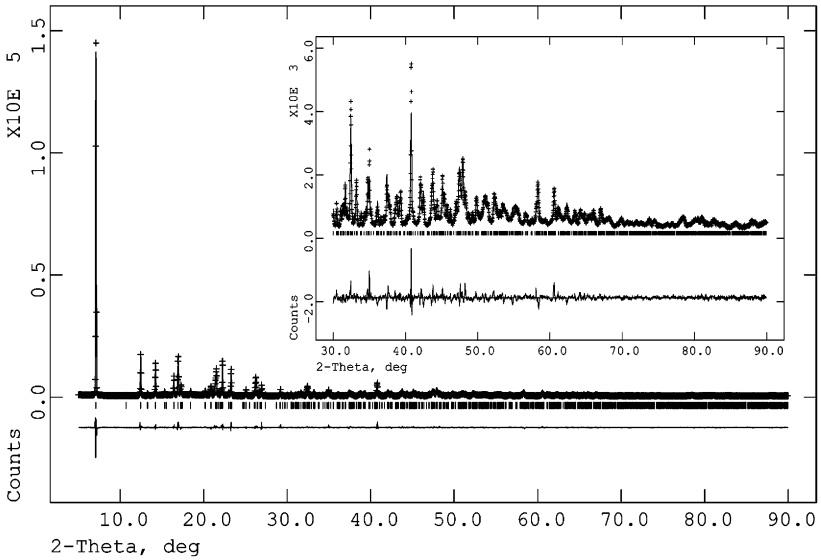

Figure 1. The final observed (crosses) calculated (lines) and difference profiles (lines) for **2**. Tick marks show reflection positions.

Table 5. Selected Hydrogen Bond Distance (Å) and Angles (deg) for 1 and 4

donor−H..acceptor	D−H	H...A	D...A	D−H...A
		1		
O4−H3..O3	1.055	2.071	3.024(5)	148.93
O4−H4..O1	1.012	2.086	3.083(6)	167.95
O5−H5..O4	0.850	2.198	2.977(8)	152.41
O5−H6..O2	0.850	2.070	2.915(8)	172.58
		4		
O2−H1..O3	0.850	2.178	3.008(3)	165.36
O2−H2..O1	0.890	1.957	2.841(3)	172.02

atoms (O1) from two different diphosphonate groups and by two water molecules (O4). These coordinated waters are involved in hydrogen bonding to the oxygen atoms (O1 and O3) of adjacent phosphonate groups. The ethylenediphosphonate groups link the chains of octahedra in the [−110] and the [001] directions, as shown in Figures 2a and 2b, to form a framework structure with a one-dimensional channel system. The channels of this framework structure run along the [100] direction and are large enough (5.66 Å [O4−O4] × 6.20 Å [C1−C1]) to locate two extraframework water molecules, O5, per unit cell. The structure and form of the chains of GaO_4F_2 octahedra linked by the tetrahedral PCO_3 moieties of the diphosphonate groups in **1** are analogous to those found in the mineral Laueite $[MnFe_2(PO_4)_2(OH)_2(H_2O)_2(H_2O)_6]$ that contains chains of $FeO_4(OH)_2$ octahedra linked by the tetrahedral PO_4 moieties.[40]

The framework structure of **1**, $Ga_2[O_3PC_2H_4PO_3](H_2O)_2F_2$, is isomeric with that found in $Ga_2[O_3PC_2H_4PO_3](H_2O)_2F_2{\cdot}H_2O$ and shown in Figure 4a.[20,21] The structures of both materials are similar as they both contain chains of corner-sharing GaO_4F_2 octahedra linked via ethylenediphosphonate groups to form framework structures containing one-dimensional channel systems. However, the GaO_4F_2 octahedra in each material are linked in a different manner, resulting in different framework structures being formed. The bridging F apexes of each GaO_4F_2 octahedra in **1** are arranged in a trans configuration about the Ga atom, as shown in Figure 3, while the bridging F apexes of

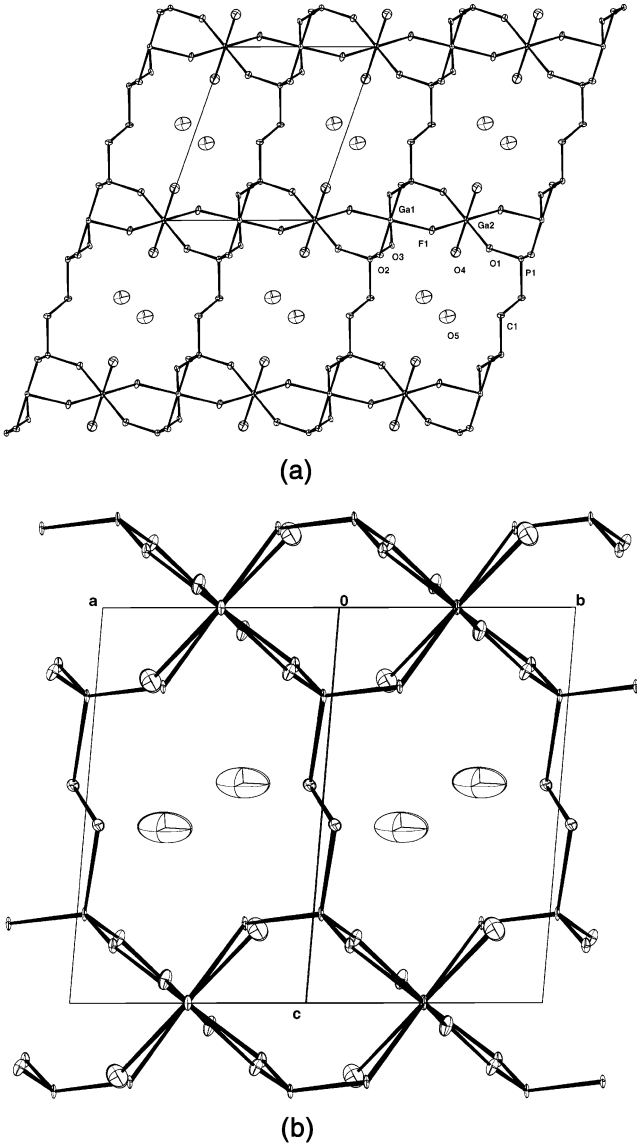

Figure 2. The structure of **1** viewed along (a) the [100] and (b) the [110] directions with thermal ellipsoids shown at 50% probability and hydrogen atoms omitted for clarity.

(40) Moore, P. B. *Am. Mineral.* **1965**, *50*, 1884.

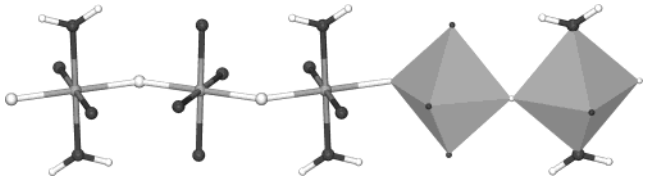

Figure 3. A ball-and-stick and polyhedral representation of the type of chain of corner-sharing Ga-centered octahedra found in the structure of compounds **1**, **2**, and **4**. Atom representation: gray balls (Ga), white balls (F), black balls (O), and small white balls (H).

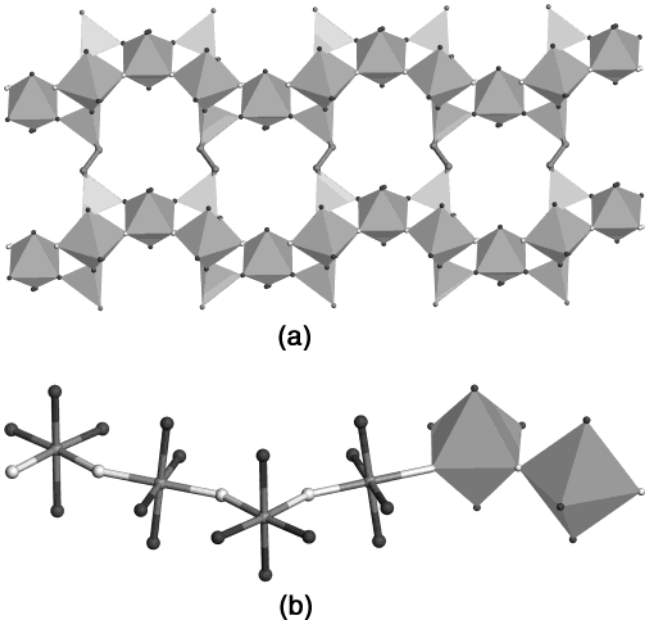

Figure 4. A polyhedral representation of the framework structure (a) and a ball-and-stick and polyhedral representation of the chain of corner-sharing Ga-centered octahedra (b) of $Ga_2[O_3PC_2H_4PO_3](H_2O)_2F_2{\cdot}H_2O$. Atom representation: gray balls (Ga), white balls (F), and black balls (O).

alternate GaO_4F_2 octahedra in $Ga_2[O_3PC_2H_4PO_3](H_2O)_2F_2{\cdot}H_2O$ are arranged in a trans and cis configuration about the Ga atom, as shown in Figure 4b. The former arrangement of GaO_4F_2 octahedra results in a relatively linear chain of octahedra, see Figure 3, while the latter arrangement forms a corrugated chain of octahedra, see Figure 4b.[20,21] The aforementioned arrangements of the GaO_4F_2 octahedra result in a greater separation of the diphosphonate units along the direction of the chains of octahedra in **1** than in $Ga_2[O_3PC_2H_4PO_3](H_2O)_2F_2{\cdot}H_2O$ and so the pore size in the former is larger than the latter. The values of the void volume as a percentage of the total volume and solvent-accessible volume are 30.7% and 30.8 Å^3 and 35.1% and 47.0 Å^3 for $Ga_2[O_3PC_2H_4PO_3](H_2O)_2F_2{\cdot}H_2O$ and **1**, respectively, reflecting the more open structure of **1** in comparison to $Ga_2[O_3PC_2H_4PO_3](H_2O)_2F_2{\cdot}H_2O$.

Structure of $Ga_2[O_3PCH_2(C_6H_4)CH_2PO_3](H_2O)_2F_2$ (2). The structure of $Ga_2[O_3PCH_2(C_6H_4)CH_2PO_3](H_2O)_2F_2$ is shown in Figure 5 and has a similar structure to **1**. The structure consists of chains of corner-sharing GaO_4F_2 octahedra with bridging fluorine atoms (F1) linking the octahedral, as shown in Figure 5a. These chains consist of two types of GaO_4F_2 octahedra that both contain gallium atoms coordinated to two fluorine atoms in a trans configuration. The remaining corners of one of the gallium-centered octahedra (Ga1) are occupied by four oxygen atoms (O4 and O1) from four different diphosphonate groups, while the remaining apexes of the other gallium-centered octahedra (Ga2) are occupied by two oxygen atoms (O3) from two different diphosphonate groups and by two water molecules (O2). The phenylenebis(methylene)diphosphonate groups link the chains of octahedra in the [−110] direction, as shown in Figure 5b, and the [001] direction, as shown in Figure 5a, to form a framework structure containing a one-dimensional channel system. The channels (8.74 Å [O2−O2] × 4.01 Å [C1−C1]) of this framework are lopsided, compared to those in structure **1**, and are too narrow, or too hydrophobic, to contain extraframework water molecules. The relative arrangement of the phenyl rings of the diphosphonate pillars within the structure result in insignificant overlap of the π systems of adjacent rings and negligible $\pi-\pi$ interactions in this system.

The ^{31}P and ^{19}F MAS SSNMR spectra of **2** (see Supporting Information) both contain one peak each centered at 16.33 and −134.53 ppm, respectively, suggesting the presence of one crystallographically independent phosphorus and fluorine site only. This is consistent with the experimentally determined crystal structure refinement using $P\bar{1}$ symmetry, but would be inconsistent with refinement using $P1$ symmetry. The chemical shifts of the two species are consistent with previously observed phosphonate groups and that observed for bridging fluorine atoms.[20,26]

The structures of **1** and **2** are closely related as both contain identical chains of corner-sharing GaO_4F_2 octahedra. The configuration of the chain of octahedra adopted in compound **2**, as opposed to the configuration adopted in $Ga_2[O_3PC_2H_4PO_3](H_2O)_2F_2{\cdot}H_2O$, arises from the inclusion of the phenylene ring in the pillaring diphosphonate group. A structure, such as that shown in Figure 4a, in which the chain of octahedra adopt the configuration in $Ga_2[O_3PC_2H_4PO_3](H_2O)_2F_2{\cdot}H_2O$, requires alternate PO_3C tetrahedra along one side of any particular chain of octahedra to point in opposite directions, i.e., left or right as shown in Figure 4a. This structural necessity makes the adoption of the type of chain of octahedra found in $Ga_2[O_3PC_2H_4PO_3](H_2O)_2F_2{\cdot}H_2O$ unlikely when the greater sized [1,4-phenylenebis(methylene)]diphosphonate group is incorporated as it would presumably require the diphosphonate group to adopt a more energetically unfavorable configuration than the one it adopts to form structure **2**. Structures **1** and **2** both contain chains of octahedra in which alternate PO_3C tetrahedra along one side of any particular chain of octahedra point in the same direction, as shown in Figure 5a. This particular configuration of the chain of octahedra will allow more freedom for the [1,4-phenylenebis(methylene)]diphosphonate groups to form a structure with a more energetically favorable configuration.

Synthesis and Characterization of the Solid-Solution Gallium Phosphite/[1,4-Phenylenebis(methylene)]diphosphonate Series: $Ga_2\{[O_3PCH_2(C_6H_4)CH_2PO_3]_{1-x}(HPO_3)_{2x}\}(H_2O)_2F_2$ ($x = 0.054$ (3), $x = 0.144$ (4) ($0 \le x \le 0.146$). The incorporation of phosphorous acid (H_3PO_3) into the initial synthesis gel in varying quantities at the expense of [1,4-phenylenebis(methylene)]diphosphonic acid led to the forma-

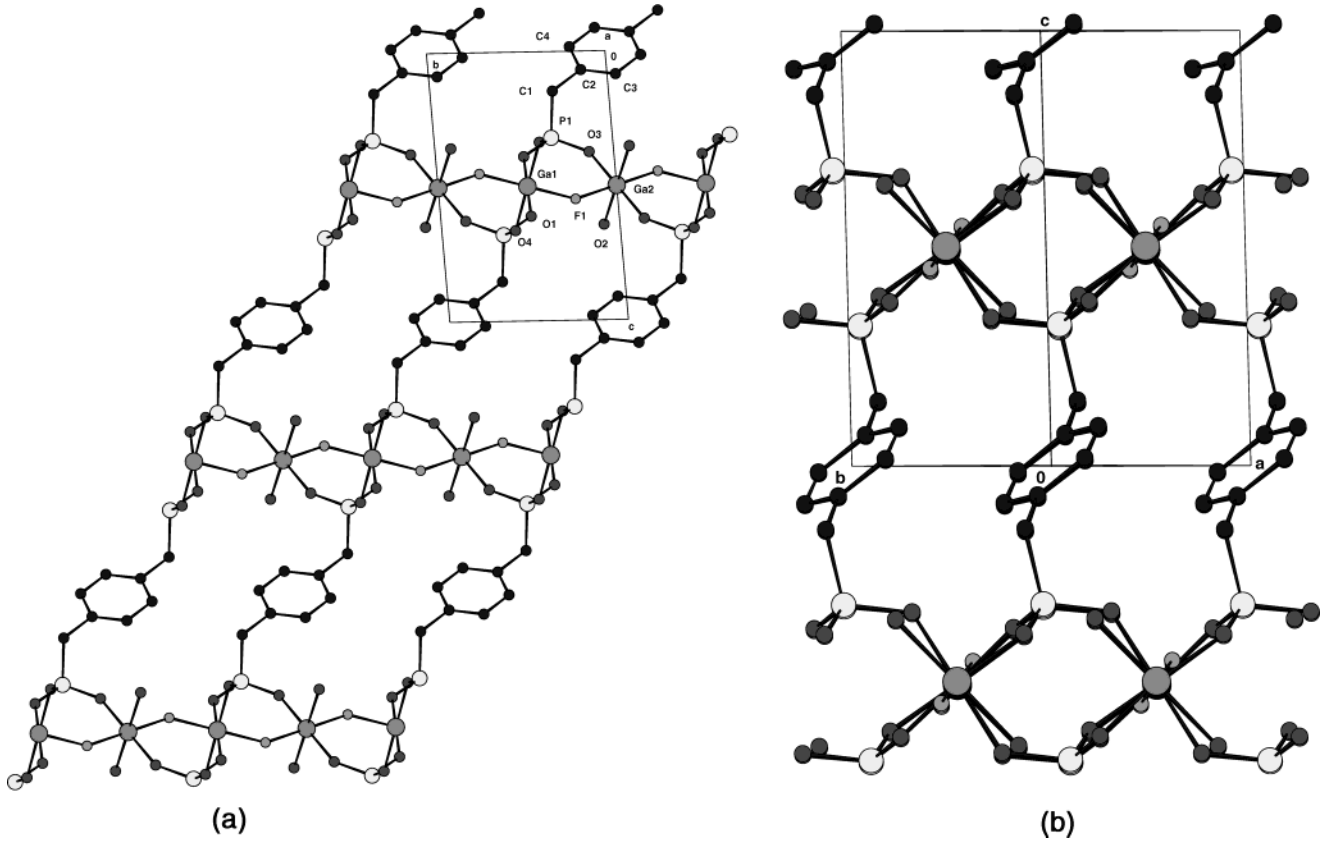

Figure 5. A ball-and-stick representation of the structure of **2** viewed along (a) the [100] and (b) the [110] directions. Hydrogen atoms omitted for clarity.

tion of crystalline powder and microcrystal materials. The ratio of the initial synthesis mixtures used are given in Table 1 and when compared to the resultant formulas obtained using other techniques indicate that approximately one-quarter of the desired substitution of the diphosphonic acid was actually achieved in the resulting solid material.

^{31}P MAS SS NMR was used to show the presence of the phosphite group in the substituted materials and to obtain a more quantative estimate of the phosphite content by comparing the ratio of the intensities of the peak, with associated spinning sidebands, of the P nuclei of the phosphite and diphosphonate groups. Figure 6 shows the ^{31}P MAS SS NMR spectra for the two phosphite-substituted materials. The spectra of the phosphite-substituted materials are identical in terms of chemical shifts and number of environments present, again indicating that the materials are monophasic. The presence of only one resonance for the diphosphonate group suggests that there is only one crystallographically independent phosphorus site in the structure of the materials. The resonance due to the ^{31}P nuclei of the diphosphonate group are centered at 16.29 ppm and that due to the ^{31}P nuclei of the phosphite group are centered at −2.92 ppm as found in other phosphite/diphosphonate solid-solution series.[17,41] The formulas of the materials derived from these ratios are given in Table 1.

The powder X-ray diffraction patterns of the materials are shown in Figure 7 and show that the substituted materials are highly crystalline, pure phase samples and their structures are based upon that of the parent framework structure. The materials are all of similar crystallinity.

The growth of microcrystals of the $x = 0.144$ phosphite-substituted sample **4** allowed the structure to be determined by single-crystal X-ray crystallographic methods. Such an accurate structure solution/refinement using single-crystal X-ray diffraction data has not been performed on any other substituted diphosphonate framework of this kind. The structure of **4** is shown in Figures 8a and 8b, where it is seen that it adopts essentially the same framework structure as that described previously for **2**. The refinement of the crystallographic occupancy of the carbon atoms in the diphosphonate linker gave a value of 0.853(6), giving a composition of $Ga_2\{[O_3PCH_2(C_6H_4)CH_2PO_3]_{0.853(6)}(HPO_3)_{0.29(1)}\}(H_2O)_2F_2$, $x = 0.147(6)$, for this phosphite-substituted phase. This value of x is in excellent agreement with the value obtained from the ^{31}P MAS SS NMR data, $x = 0.144(5)$. The major difference between the structures of **2** and **4** is that phosphite groups substitute 14.7% of the diphosphonate pillars, each diphosphonate group being replaced by two phosphite groups as seen in Figures 8a and 8b. The distance between adjacent diphosphonate groups where the diphosphonate pillars are replaced is 14.16 Å in the [001] direction (C4−C4 11.43 Å for the closest points of the pillars), as seen in Figure 8a, and 9.92 Å in the [−110] direction, as seen in Figure 8b. As the substitution of the diphosphonate groups is random, the formation of a larger pore running throughout the whole structure is unlikely as this would require the phosphite

(41) Scott, K. J.; Zhang, Y.; Wang, R. C.; Clearfield, A. *Chem. Mater.* **1995**, *7*, 1095.

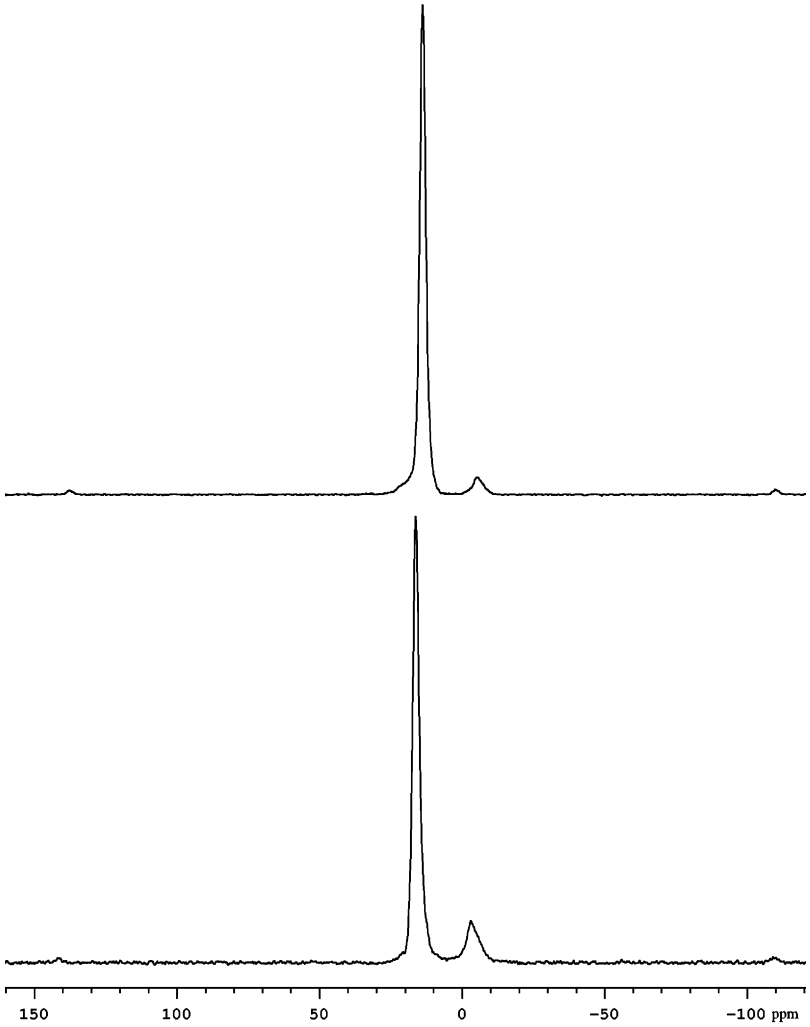

Figure 6. The ^{31}P MAS SSNMR spectra of $Ga_2[(O_3PCH_2(C_6H_4)CH_2PO_3)_{1-x}(HPO_3)_{2x}](H_2O)_2F_2$: $x = 0.054$ (**3**) (top) and $x = 0.144$ (**4**) (bottom).

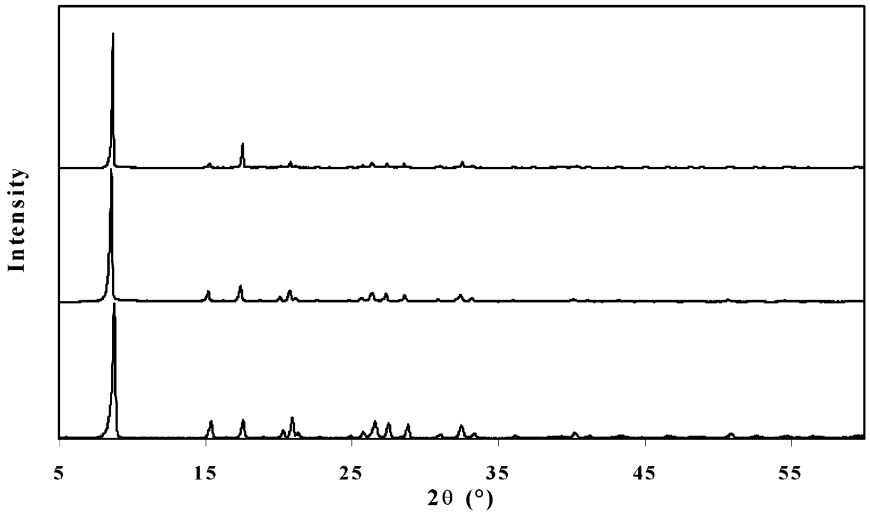

Figure 7. The normalized powder X-ray diffraction patterns of $Ga_2[(O_3PCH_2(C_6H_4)CH_2PO_3)_{1-x}(HPO_3)_{2x}](H_2O)_2F_2$: $x = 0$ (**2**) (bottom), $x = 0.054$ (**3**) (middle), and $x = 0.144$ (**4**) (top).

groups to be incorporated into the material in an ordered manner. However, the structure now contains larger apertures randomly arranged throughout the structure, making it more open. These crystallographic results indicate that the phosphite substitution leads to an increase in the overall porosity, or openness, of the material. The size of the apertures is the largest observed in this family of group 13 metal diphosphonates.

The TGA traces of ($x = 0$) **2**, ($x = 0.541$) **3**, and ($x = 0.144$) **4** are shown in Figure 9. Four main mass loss stages are observed in the TGA trace of the decomposi-

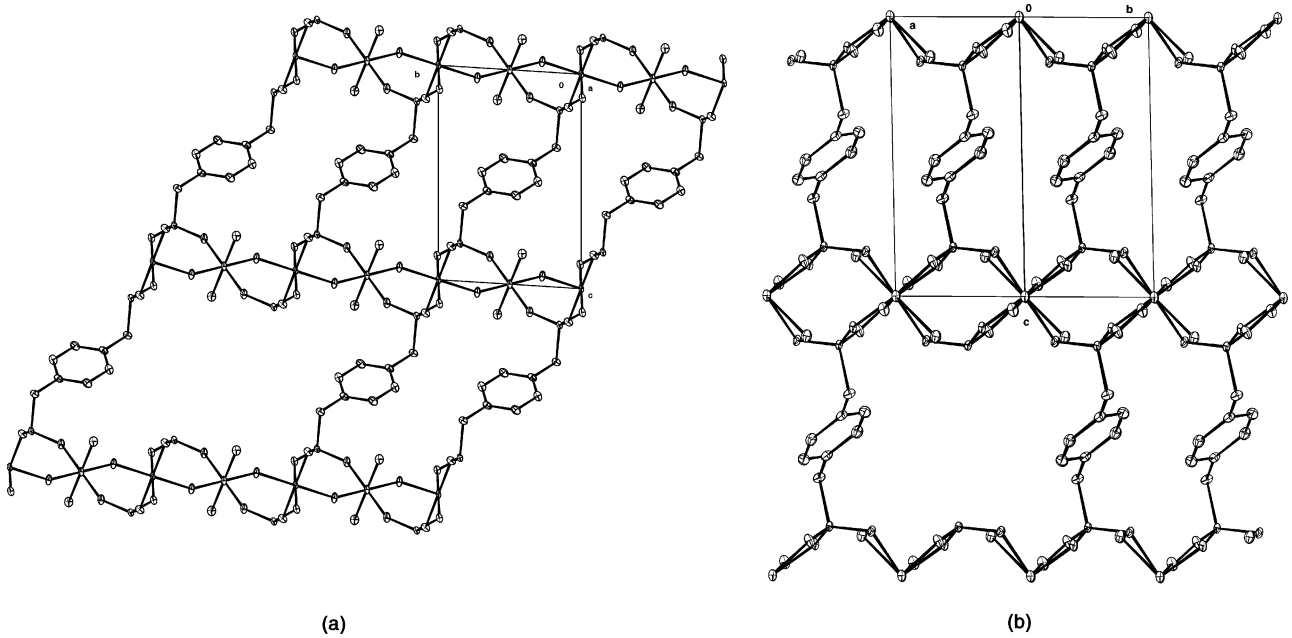

Figure 8. The structure of **4** viewed along (a) the [100] and (b) the [110] directions with thermal ellipsoids shown at 50% probability and hydrogen atoms omitted for clarity.

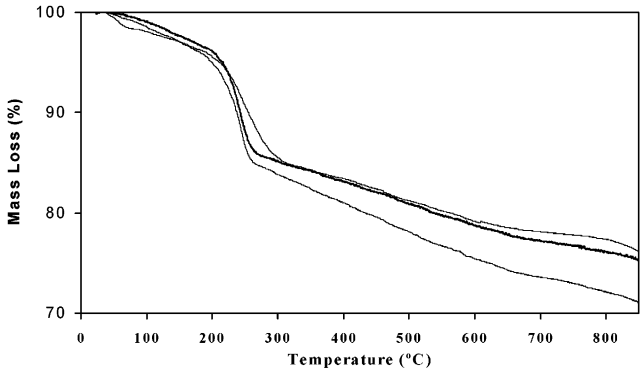

Figure 9. The TGA trace of the mass loss of $Ga_2[(O_3PCH_2(C_6H_4)CH_2PO_3)_{1-x}(HPO_3)_{2x}](H_2O)_2F_2$: $x = 0$ (**2**) (top, thin line), $x = 0.054$ (**3**) (middle, thick line), and $x = 0.144$ (**4**) (bottom, thin line).

tion of $Ga_2[O_3PCH_2(C_6H_4)CH_2PO_3](H_2O)_2F_2$ (**2**). The first mass loss occurs over the temperature range from 30 to 80 °C and has a magnitude of 1.66%. This loss is attributed to the removal of surface water. The second mass loss occurs between 80 and 200 °C and has a magnitude of 2.29% and the third, most rapid, mass loss occurs between 200 and 317 °C and has a magnitude of 11.37%. These two mass losses are attributed to the loss of the coordinated water molecules and fluorine atoms (calculated 15.96%). The fourth mass loss occurs slowly over the temperature range 317−850 °C and has a magnitude of 8.58%. This loss is assigned to the decomposition of the [1,4-phenylenebis(methylene)]-diphosphonate linkage (calculated 22.8%). The magnitude of this loss is less than expected for full decomposition of the [1,4-phenylenebis(methylene)]diphosphonate linkages, indicating that the organic component is not fully oxidized and removed in the experiment.

The mass change curves for ($x = 0.541$) **3** and ($x = 0.144$) **4** show the same main mass losses as sample ($x = 0$) **2**, except that they show no trace of any surface water loss. However, comparison of the three mass loss traces indicates that the temperature at which the framework water and fluorine atoms are removed decreases and the degree of mass loss attributed to the removal of the organic portion of the diphosphonate groups increases in the order of increasing phosphite substitution in the samples. Both these observations are accounted for by considering the increase in porosity of the material upon increasing the degree of phosphite substitution. As more diphosphonate pillars are replaced by phosphite groups, the internal volume of the material will become more open, allowing for easier diffusion throughout the solid of the framework species being removed, resulting in desorption and decomposition at lower temperatures and to a greater degree.

Conclusions

In this work we have shown that the configuration adopted by the constituent inorganic chains within the framework materials of general formula $Ga_2[O_3PRPO_3](H_2O)_2F_2$ can be directed by control of the reaction conditions or the form of the organic constituent. When R = the ethylene group, control of the pH and duration of the reaction lead to formation of $Ga_2[O_3PC_2H_4PO_3](H_2O)_2F_2{\cdot}2H_2O$ (**1**) that contains linear chains of corner-sharing GaO_4F_2 octahedra and has a more open framework structure than the related phase, $Ga_2[O_3PC_2H_4PO_3](H_2O)_2F_2{\cdot}H_2O$, which contains corrugated chains of corner-sharing GaO_4F_2 octahedra. When R = the 1, 4-phenylenebis(methylene) group, the framework material $Ga_2[O_3PCH_2(C_6H_4)CH_2PO_3](H_2O)_2F_2$ is formed in which the large, potentially functionalizable, phenylene groups cause the linear arrangement of the corner-sharing GaO_4F_2 octahedra in the chains to be adopted. This framework material is nonporous in its pure form but substitution of some of the diphosphonate groups for phosphite groups in the initial preparation of the materials leads to the formation of members of the solid-solution series $Ga_2\{[O_3PCH_2(C_6H_4)CH_2PO_3]_{1-x}(HPO_3)_{2x}\}(H_2O)_2F_2$ ($0 \le x \le 0.146$) that have more open structures and contain the largest apertures reported in the family of group 13 metal diphosphonate materials. The forma-

tion of these materials exemplify how this type of approach to control the form of the inorganic component in the resultant material, in combination with the control of the organic component, provides a potent methodology for the full rational design of the structure and functionality of organic−inorganic hybrid materials.

Acknowledgment. The authors thank Dr. A. Aliev (ULIRS), Dr. M. Odlyha (ULIRS), and Dr. A. Beard for collection of the SS MAS NMR, TGA, and microprobe data, respectively, Dr. D. Apperley of the EPSRC Solid State NMR Service, University of Durham, U.K., for collection of ^{31}P SSNMR spectra of **3** and **4**, Dr. S. J. Teat for help in collection of the single-crystal X-ray diffraction data for sample **4**, and the EPSRC National Crystallography Service, University of Southampton, U.K., for collecting single-crystal X-ray data for compound **1**. M.P.A. thanks the Royal Society for provision of a University Research Fellowship and H.G.H. thanks EPSRC for provision of a quota award and for funding.

Supporting Information Available: The ^{31}P and ^{19}F MAS SSNMR spectra of compound **2** and the CIF files for compounds **1**, **2**, and **4**. This material is available free of charge via the Internet at http://pubs.acs.org.

CM049607V